

## Defect detection in pipes based on the measurement of surface displacements

Philip BECHT<sup>1</sup>, Elke DECKERS<sup>1</sup>, Claus CLAEYS<sup>1</sup>, Bert PLUYMERS<sup>1</sup>, Wim DESMET<sup>1</sup>

<sup>1</sup> Dept. of Mechanical Engineering, PMA division – member of Flanders Make, KU Leuven.  
Celestijnenlaan 300, box 2420, 3001 Leuven (Heverlee), BELGIUM  
[Philip.Becht@kuleuven.be](mailto:Philip.Becht@kuleuven.be)

### Key words:

Guided wave, defect detection, multi-mode scattering

### Abstract

*This paper describes a novel guided wave technique for the detection of inhomogeneities in pipes, which is not relying on the excitation of one specific wavemode. The method works in the frequency domain and can be divided into three steps: (i) measurement of the surface-displacement of a pipe that is excited by an unknown combination of wavemodes at one discrete frequency, (ii) localization of the defect based on the surface-displacement, (iii) fitting the measured surface-displacement in the pipe-section in front of and behind the defect with a set of possible wavemodes. After this step, the contribution of every wavemode to the displacement-field and thus the wave-scattering of the incident modes at the defect is known. The technique is applied in a numerical model to analyze pipes with and without defect and to study the influence of the number of measurements used for the calculation of the scattering matrix and the presence of a random measurement error.*

## 1 INTRODUCTION

Undetected defects in pipes or pipe-like structures can cause severe environmental and economic damage and be hazardous for human life and safety. One example is an unscheduled four-days shutdown of a pipeline in Alaska in January 2011, capable of transporting up to 650 000 barrels of oil per day. As a consequence the price of oil rose by \$4 per barrel [1]. The reason for unexpected defects are versatile and vary from fatigue due to vibration over corrosion [2] to uncertainties in the long-term behavior of new high performance materials [3].

Within the last 20 to 30 years the ultrasonic guided wave method for pipe inspection has been intensively studied and successfully applied to detect, localize and specify defects in pipes. This method uses the dispersive behavior of waves in solid material, which means that different wavemodes propagate at different velocity. If only one discrete wavemode is excited, its reflection and/or transmission at/through a defect and possible conversion to other wavemodes can be measured due to the difference in time of flight between measuring position and defect. The applied excitation is of importance, as indicated by the large amount of research that has been conducted in this field, see e.g. [4-6]. Those papers concentrate on the excitation of the axisymmetric torsional and longitudinal modes. Therefore mainly the reflection and transmission behavior of those wavemodes at differently shaped defects has been studied so far [2, 7-11]. Demma et al. [11] showed, that the detection and specification of relatively simply

shaped defects in pipes is possible, when combining the available research findings. However, the detection and specification of complex, realistically shaped defects is significantly more challenging, as indicated by Carandente and Cawley [2]. Furthermore Carandete, Ma and Cawley studied the influence of the slope of a tapered defect and found that due to reflection from the start and the end of the taper the interpretation of the measured reflected signal becomes more complex than for simply shaped defects [10].

As can be concluded from the previous paragraph, ultrasonic guided waves comprise a big potential for the detection of defects in pipes, but especially the results of [2] show that the available information is not always sufficient to specify real life defects. Additional information could be generated from the scattering behavior of additional incident modes. Following the current approach in time domain, this would lead to overlapping contributions of different wavemodes in the reflected signal. Although this problem has already been addressed (most recently by Kim and Park [12]), having multiple incident wavemodes at the same time would still be a major issue for the calculation of transmission and reflection coefficients. The reason is that it would not be possible to distinguish the contribution of the reflected or transmitted incident wavemode and the contribution of mode conversion from other incident wavemodes to the measured reflected or transmitted signal.

The aim of this paper is to present a technique that is capable of calculating a complete scattering matrix for all propagating modes based on multiple measurements of surface displacements of a pipe, while the excitation at each measurement can be unknown, but must be linearly independent from the excitation used in the other measurements. Using this strategy, also the scattering behavior of higher order incident modes can be used for defect detection and the complexity to produce only one propagating mode as excitation can be overcome.

After introducing this technique, a numerical study on the influence of uncertainties on the correctness of the obtained scattering matrix is presented.

## 2 CALCULATION OF SCATTERING MATRIX BASED ON THE MEASUREMENT OF SURFACE DISPLACEMENTS

A pipe of infinite length containing exactly one defect is assumed. It is sectioned in a finite domain left of the defect  $\Omega_1$ , the finite domain of the defect  $\Omega_D$  and a finite domain at the right of the defect  $\Omega_2$ , as shown in Figure 1.

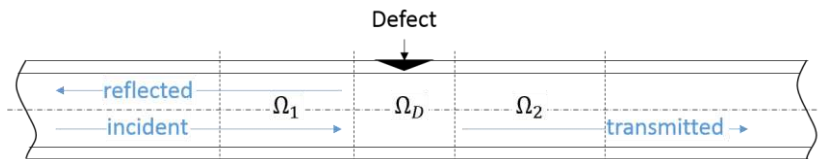


Figure 1: Separation of pipe in domains

The pipe is harmonically excited at an axial position sufficiently far to the left from  $\Omega_1$ , so that the influence of the excitation on the displacements in  $\Omega_1$  can be resembled by a superposition of only propagating wavemodes with arbitrary amplitude and phase. Those wavemodes are from now on referred to as incident wavemodes  $\Phi^{inc}$ . At the defect the incident wavemodes can be reflected to  $\Omega_1$  or transmitted to  $\Omega_2$ . Also a mode conversion of incident modes to reflected or transmitted propagating, evanescent or decaying wavemodes is possible. The resulting displacement  $q_1$  and  $q_2$  in  $\Omega_1$  and  $\Omega_2$ , respectively, is the superposition of all possible wavemodes in the respective domain ( $\Phi^{inc}, \Phi^{ref}, \Phi^{trans}$ ) times their wave contribution factors ( $a^{inc}, a^{ref}, a^{trans}$ ). Here the superscripts 'inc' and 'ref' refer to the incident and reflected waves in  $\Omega_1$  and the superscript 'trans' refers to the transmitted waves

in  $\Omega_2$ :

$$q_1 = [\Phi^{inc} \quad \Phi^{ref}] \begin{bmatrix} a^{inc} \\ a^{ref} \end{bmatrix}, \quad (1)$$

$$q_2 = \Phi^{trans} a^{trans}.$$

To calculate the scattering matrix of all incident modes, the surface displacement of sections  $\Omega_1$ ,  $\Omega_D$  and  $\Omega_2$  must be measured at one excitation. Since it is assumed, that the position of the defect is unknown at this time, first the measured part of the pipe must be split in the above described domains  $\Omega_1$ ,  $\Omega_D$  and  $\Omega_2$ . In case of a severe defect, its position might already be visible by visualizing the measured displacements, yet in a more general case this does not hold. It has been observed that  $\Omega_1$  and  $\Omega_2$  can be identified following the approach introduced below.

Neglecting the possible presence of a defect and treating the entire measured region as one domain, the measured surface displacement  $q_{1,D,2,surf} = q_{1,surf} \cup q_{D,surf} \cup q_{2,surf}$  in this domain can be represented as a superposition of propagating wavemodes in positive and negative axial direction  $\Phi_{surf}^{+/-}$  times their contribution factors  $a^{+/-}$ , so that

$$q_{1,D,2,surf} = [\Phi_{surf}^+ \quad \Phi_{surf}^-] \begin{bmatrix} a^+ \\ a^- \end{bmatrix}. \quad (2)$$

The subscript ‘surf’ implies, that only the displacement components on the surface of the pipe are considered, as only these can be measured.

As an infinite pipe is assumed, reflection of the incident waves at a finite end can be ruled out, which is why  $a^-$  should be equal to  $\mathbf{0}$  if there is no defect.

(2) can be solved for the unknown wave contribution factors  $a^{+/-}$  and used for the calculation of a fitting error  $e_{fit}$ :

$$e_{fit} = q_{1,D,2,surf} - [\Phi_{surf}^+ \quad \Phi_{surf}^-][\Phi_{surf}^+ \quad \Phi_{surf}^-]^\dagger q_{1,D,2,surf}, \quad (3)$$

where the superscript  $\dagger$  indicates the pseudo inverse of a matrix.

Visualizing  $e_{fit}$  on the complete surfaces enables the separation of the measured surface in one domain of incident and reflected wavemodes and one domain of transmitted wavemodes.

Once the boundaries of  $\Omega_1$  and  $\Omega_2$  are known, the wave contribution factors for the incident, the reflected and the transmitted wavemodes  $a^{inc}$ ,  $a^{ref}$  and  $a^{trans}$  can be calculated similarly using (1) but adapting it to the fact that only surface displacements can be measured ( $q_1 = q_{1,surf}$ ,  $q_2 = q_{2,surf}$ ,  $\Phi^{inc} = \Phi_{surf}^{inc}$ ,  $\Phi^{ref} = \Phi_{surf}^{ref}$ ,  $\Phi^{trans} = \Phi_{surf}^{trans}$ ).

Applying the steps presented so far, it is possible to calculate the wave contribution factors of all wavemodes with non-negligible surface displacement in  $\Omega_1$  and  $\Omega_2$  for an unknown excitation.

The interaction between the incident, reflected and transmitted waves at a discrete frequency can be expressed in terms of a scattering matrix  $s$ .  $s$  is intrinsic to a defect, which means there is no dependency on the excitation (here represented by  $a^{inc}$ ):

$$\begin{bmatrix} a^{ref} \\ a^{trans} \end{bmatrix} = s a^{inc}. \quad (4)$$

$s$  is a matrix of the dimensions  $2(n+m) \times n$ , where  $n$  is the number of propagating wavemodes and  $m$  the number of evanescent and decaying wavemodes in positive or negative axial direction, respectively. Since the pipe itself is axisymmetric and the cross section of  $\Omega_1$

and  $\Omega_2$  are equal, also the number of waves propagating in positive and negative axial direction in  $\Omega_1$  and  $\Omega_2$  is equal.

Calculating the wave contribution factors for  $k$  measurements results in  $k$  sets of wave contribution factors that can be grouped in the matrices

$$A^{inc/ref/trans} = [a_1^{inc/ref/trans} \quad a_2^{inc/ref/trans} \quad \dots \quad a_k^{inc/ref/trans}]. \quad (5)$$

Supposing that  $\det A^{inc} \neq 0$ , which can be achieved by  $k = n$  linearly independent types of excitation, the scattering matrix  $s$  can be calculated:

$$s = \begin{bmatrix} A^{ref} \\ A^{trans} \end{bmatrix} A^{inc}{}^{-1}. \quad (6)$$

With the superscript -1 being the inverse of a matrix. The minimum number of linearly independent excitations  $k = n$  results from the fact that  $A^{inc}$  depicts excitations far away from the left boundary of  $\Omega_1$  and contains therefore only propagating wavemodes. An overdetermined system of equations containing a higher number of measurements can be processed by using a pseudo inverse instead of a regular inverse to invert the matrix  $A^{inc}$ .

Compared to other guided wave methods, the main novelty here is that from (6) the scattering behavior of all incident wavemodes can be obtained, whereas traditionally only the scattering of one or two incident wavemodes to a limited number of reflected wavemodes is investigated.

### 3 NUMERICAL IMPLEMENTATION

#### 3.1 Wave and Finite Element Model

To calculate the possible wavemodes in  $\Omega_1$  and  $\Omega_2$  the two-dimensional Wave and Finite Element Method (WFEM) is applied. The implementation is done following the description given by Manconi and Mace [13]. The formulation has been validated against an analytical solution [14] and the same approach has been successfully compared to a FE model of a finite structure [15].

The implemented WFEM allows calculation of displacement wavemodes  $\Phi$  at a discrete frequency and spatial position and to propagate these wavemodes in axial and circumferential direction. For further information the reader is referred to [13].

#### 3.2 Hybrid WFEM/FEM

In order to analyze the influence of uncertainties on the quality of the scattering matrix obtained from the measurement of surface displacements, a numerical model of an infinite pipe with a defect is used. The cross section of the pipe in the vicinity of the defect ( $\Omega_D$  in Figure 1) is modelled by means of FEM. Two semi-infinite waveguides ( $\Omega_1$  and  $\Omega_2$ ) are attached to the left and the right of the defected pipe model, while the physical properties of these domains are described in terms of wavemodes and their corresponding wave contribution factors. Details about the hybrid WFEM/FEM can be found in [16] and [17], where the coupling and the underlying assumptions are discussed and practical examples are given.

The chosen modelling technique is rather fast and once the scattering matrix of a defect is known, virtual measurements of the surface displacement due to different excitations (expressed in terms of different contribution factors of the incident wavemodes  $a_{inc}$ ) can easily be calculated following (1) and (4), only evaluating the nodal displacements on the surface. Furthermore,  $s$  is directly calculated and can be used later on to determine the correctness of

the scattering matrix predicted based on the approach described in chapter 2.

## 4 NUMERICAL STUDY

### 4.1 Specification of test case

A DN80 steel pipe ( $E = 2.1 \cdot 10^{11} \text{Pa}$ ,  $\eta = 0.29$ ,  $\rho = 7850 \text{ kg/m}^3$ ) with 88.9mm outer diameter and 3.2mm wall thickness is modelled using 4 linear solid elements in wall thickness direction (1mm axial dimension,  $1.2^\circ$  circumferential dimension). The scattering matrices for a pipe without defect and one with a through thickness defect, ranging from  $0^\circ$  to  $13.2^\circ$  in circumferential direction and no axial extent is calculated. The defect is modelled by detaching nodes. Simulations for both models are performed with 59 different circumferential wavemodes. The difference in the scattering matrix between a simulation with 57 and one with 59 different circumferential wavemodes is maximum  $3 \cdot 10^{-5}\%$  of the maximum value of the scattering matrix at 15kHz. Therefore convergence is achieved.

The surface displacements for different excitations are simulated for both cases. The implementation of the excitation in MATLAB is done by generating a random real and imaginary part for the wave contribution factor  $a_{inc}$  of each propagating incident wavemode using MATLAB's rand command. To allow the comparison of the findings made in this research to an experimental setup using shaker excitation, the excitation frequency is chosen to be 15kHz. This is far below the center frequencies usually used in guided wave defect detection, but as will be shown the presence of a defect can also be detected at this comparatively low frequency.

The highest order circumferential wavenumber of a propagating wavemode in axial direction for the given pipe at 15kHz is  $k_\theta = 6 (2\pi)^{-1}$ . To facilitate the reading, the unit  $(2\pi)^{-1}$  of the circumferential wavenumber is omitted from here onwards. The propagating wavemode with the shortest wavelength in axial direction is the flexural mode at  $k_\theta = 3$  with a wavelength of  $\lambda = 7\text{cm}$ . Based on these properties, the mesh grid of the simulated surface displacement measurements is defined by one measurement point every 5mm in axial direction and 1 measurement point every  $6^\circ$  in circumferential direction. This yields at least 14 measurement points per wavelength in axial direction and 10 measurement points per wavelength in circumferential direction, which is sufficient to capture a sinewave. The axial extent of  $\Omega_1$  and  $\Omega_2$  is defined as 0.2m.

### 4.2 Definition of evaluation criterion

Although in theory the detection of evanescent and decaying wavemodes is possible using the method presented in this paper, the relatively coarse mesh grid does not provide a sufficient number of data points for the identification of rapidly decaying or evanescent waves. Therefore, and because the influence of the evanescent modes is mainly concentrated on the area near the boundary of  $\Omega_1$  and  $\Omega_2$  to  $\Omega_D$ , the study undertaken here focuses on the scattering behavior of propagating wavemodes only. Furthermore only radial displacement components are taken into account, as in reality these are relatively easy to measure. Since the propagating 0-order torsional wavemode contains almost no radial displacement components, also this mode cannot be detected and is therefore eliminated from the wave mode set described in chapter 2.

Figure 2 shows the reflection, transmission and mode conversion of an incident wavemode at a pipe without defect (left) and at a pipe with a  $13.2^\circ$  defect (right). The x-axis represents

the absolute value of the amplitude of the incident wavemodes in the order presented in Table 1. The y-axis contains the absolute value of the amplitude of the reflected and transmitted modes, respectively, relative to the amplitude of the incident wavemodes. These modes are listed in the same order (Table 1). Thus the diagonal with value 1 in the transmission coefficient of the model with no defect (Figure 2 top left) means that all incident modes are transmitted to 100%. Since all other elements in this matrix are 0, there is no mode-conversion in this case. Also the coefficients for the reflection at a pipe without defect (bottom left) are 0, which implies that there is, as expected, no reflection.

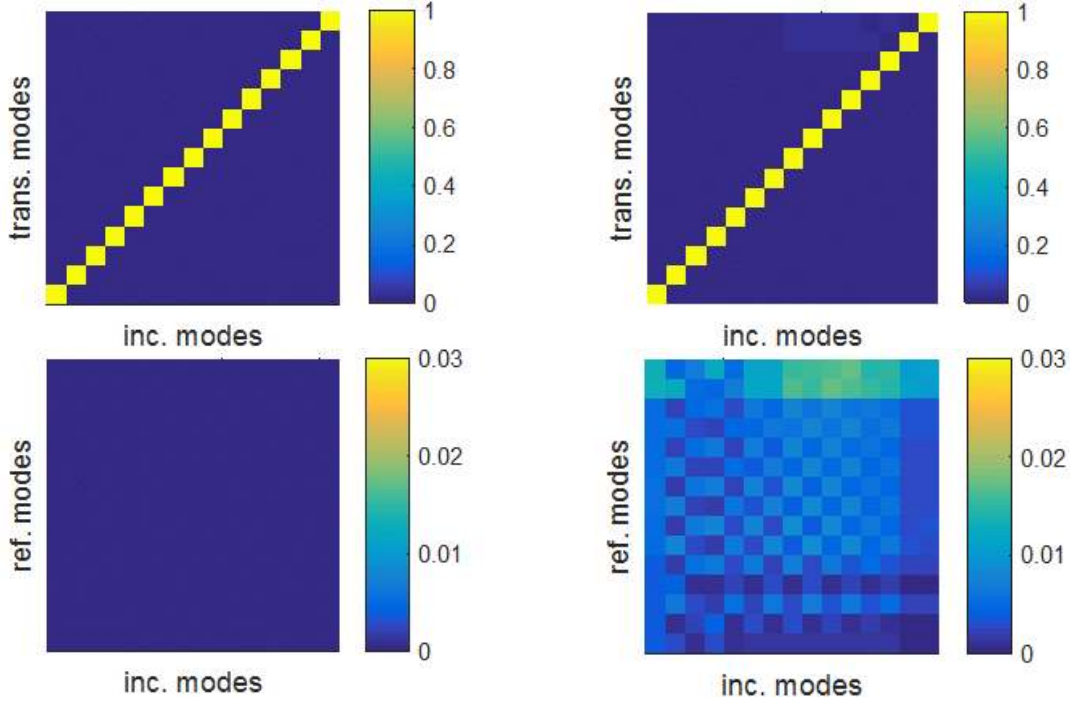


Figure 2: Scattering matrix for a pipe without defect (left) and with a 13.2° defect (right), split up in transmission (top) and reflection (bottom)

Number of mode in scattering matrix	Circumferential wavenumber	Main displacement component
1	$k_{\theta} = 0$	Longitudinal
2	$k_{\theta} = +1$	Longitudinal
3	$k_{\theta} = +1$	Radial
4	$k_{\theta} = -1$	Longitudinal
5	$k_{\theta} = -1$	Radial
6	$k_{\theta} = +2$	Radial
7	$k_{\theta} = -2$	Radial
8	$k_{\theta} = +3$	Radial
9	$k_{\theta} = -3$	Radial
10	$k_{\theta} = +4$	Radial
11	$k_{\theta} = -4$	Radial
12	$k_{\theta} = +5$	Radial
13	$k_{\theta} = -5$	Radial
14	$k_{\theta} = +6$	Radial
15	$k_{\theta} = -6$	Radial

Table 1: Numbering of propagating wavemodes in DN80 pipe with 3.2mm wall thickness at 15kHz (corresponding to the scattering matrices presented in Figure 2).

Also the transmission matrix of the model with a  $13.2^\circ$  defect in circumferential direction (Figure 2, top right) shows clearly a dominant transmission of the incident modes (diagonal). But in contrast to the pipe without defect, here an additional mode conversion mainly to the modes  $k_\theta = \pm 6$  occurs. This mode conversion to the propagating modes with  $k_\theta = \pm 6$  can also be observed in the reflection matrix (bottom right).

Linking the scattering matrix with size, orientation and type of defects is the aim of upcoming research. Nevertheless, a strong mode conversion can be seen in the presented example, especially for reflection, as well as for transmission of the incident  $k_\theta = \pm 4$  to the reflected and transmitted  $k_\theta = \pm 6$ . Because this property reacts very sensitive to this type of defect, it is used to quantify the quality of the scattering matrix obtained from the measurements of surface displacements.

### 4.3 Influence of parameters

In the following a study on the influence of the parameters

- Number of measurements to calculate the scattering matrix ( $k$  in Chapter 2)
- Measurement error

on the quality of the scattering matrix is presented.

#### 4.3.1 Number of measurements

In total 48 measurements with different excitations are simulated and their surface displacement is calculated. For each mark in Figure 3,  $k$  measurements are grouped and the reflection coefficients of the  $k_\theta = 4$  mode to the  $k_\theta = 6$  mode is predicted following the procedure described in chapter 2. In order to assure a sufficient amount of new information for the prediction of additional reflection coefficients, in each case 3 new measurements are included and the first 3 measurements are omitted. This means e.g. for  $k = 15$  that the first mark is calculated based on the virtual measurements 1-15, mark 2 based on virtual measurements 4-18, mark 3 based on virtual measurements 7-21, ...

From Figure 3, it can be seen that the reflection coefficient for the pipe without defect (red circles) is predicted correctly, independent of the number of linearly independent measurements. In contrast, the reflection coefficient for the pipe with defect (blue crosses) calculated from ‘measured’ radial surface displacements is clearly influenced by the number of measurements included in the calculation. A big spreading, when repeating the procedure with different measurements can be observed for the coefficients calculated based on the minimally required number of measurements  $k = n = 15$  (16 propagating wavemodes minus 1 propagating torsional wavemode, which cannot be detected from a measurement of radial displacements). This spreading rapidly reduces with increasing number of measurements used for the calculation of the scattering matrix, so that at  $k = 2n = 30$  the standard deviation is almost 0 and the reflection coefficient converges to the correct value.

Similar behavior can be observed for the reflection of the  $k_\theta = -4$  mode to the  $k_\theta = -6$  mode and the transmission of the  $k_\theta = \pm 4$  modes to the  $k_\theta = \pm 6$  modes, which are not presented separately in this paper.

From (6) it can be deduced that the calculated scattering matrix should be predicted exactly (apart from numerical errors) if 15 or more measurements are taken into account. As can be seen from Figure 3, this holds for the pipe without defect, but is clearly not the case for the defected pipe, where the accuracy and repeatability of the predicted scattering matrix increase with the number of measurements used for the calculation. This can be explained amongst others by the mode conversion of the incident first torsional mode to modes with radial

displacement components at the defect. Furthermore, also the mode conversion of all incident modes to decaying and evanescent waves (in this study not included in the wavemodes  $\Phi^{inc}$ ,  $\Phi^{ref}$ ,  $\Phi^{trans}$ ) can lead to inaccuracies in the vicinity of the defect.

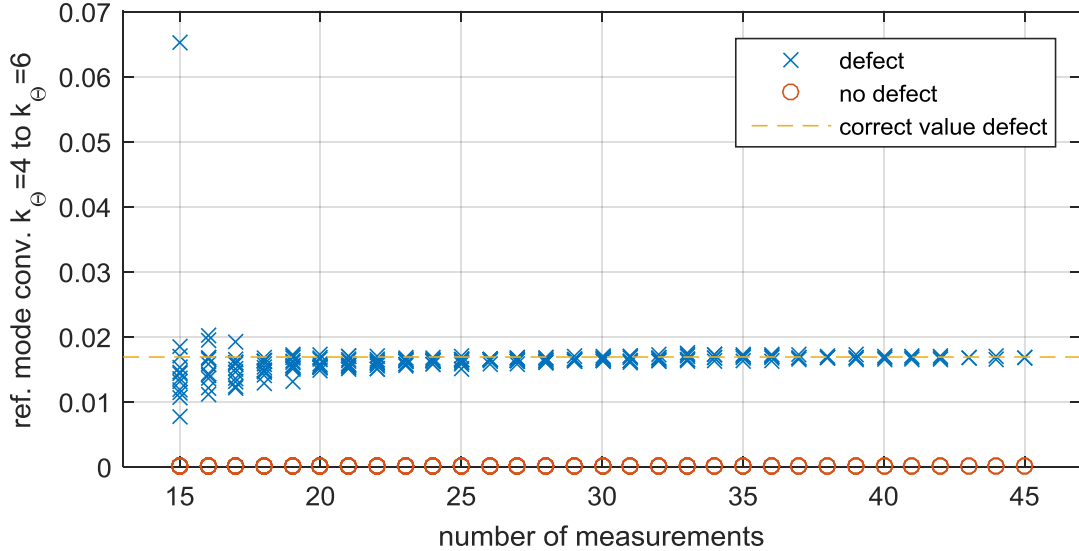


Figure 3: Reflection coefficient from the incident  $k_\theta = 4$  mode to the  $k_\theta = 6$  mode depending on the number of virtual measurements used for calculating the scattering matrix.

The conclusion that can be drawn from this observation is that even if all of the inaccuracies in measurement and process can be excluded, the number of measurements used for the calculation of a scattering matrix should be higher than the theoretical minimum. The absolute number needed depends on the desired prediction accuracy and the influence of other parameters, such as errors and can therefore not be generally determined.

### 4.3.1 Measurement error

In this section the influence of a random measurement error at each measurement point is discussed. The error is implemented by adding a random displacement to the calculated displacement at each measurement point. The vector of random displacements is created using MATLAB's `randn` command. In order to study the influence of the error, the standard deviation is specified as roughly 0.1%, 0.5%, 1% and 5% of the maximum surface displacement of one virtual measurement. It should be emphasized that e.g. at an error level with a standard deviation of 5% in some measurements the maximum error constituted up to 40% of the maximum displacement.

In Figure 4 the reflection coefficients of the  $k_\theta = 4$  mode to the  $k_\theta = 6$  mode at 4 different levels of measurement error are displayed. As discussed before, the accuracy of the predicted transmission and reflection coefficients based on 30 measurements without any measurement error is close to the correct value. Therefore the reflection coefficients based on 30 measurements with different noise levels are calculated and compared. In addition the reflection coefficients of scattering matrices calculated based on 20 measurements are presented in Figure 4 in order to compare the influence of measurement errors in combination with a change in the number of measurements.

At the figure relating to an error of 0.1% standard deviation (top left), there is no significant inaccuracy added by the error. When increasing the error to 0.5% standard deviation (top right),

the predicted reflection coefficients tend to spread in a wider range for both, the pipe with and without defect. This trend continues (bottom left, error of 1% standard deviation) until at an error of 5% standard deviation (bottom right) the predicted reflection coefficients for a pipe with and without defect start to blur into each other. Thus, the distinction between pipes with the modelled defect and without defect cannot be made anymore at this amount of noise and only 20 measurements.

The general observation that repeatability and accuracy of the scattering matrix calculated based on measured surface displacements increase with the number of measurements included in the calculation can be verified looking at Figure 4. The inaccuracy due to measurement errors for the pipe with defect is in the same order of magnitude as the inaccuracy at a low number of measurements. Other than in Figure 3, also the predicted reflection coefficients in the case without defect spread when assuming a random measurement error.

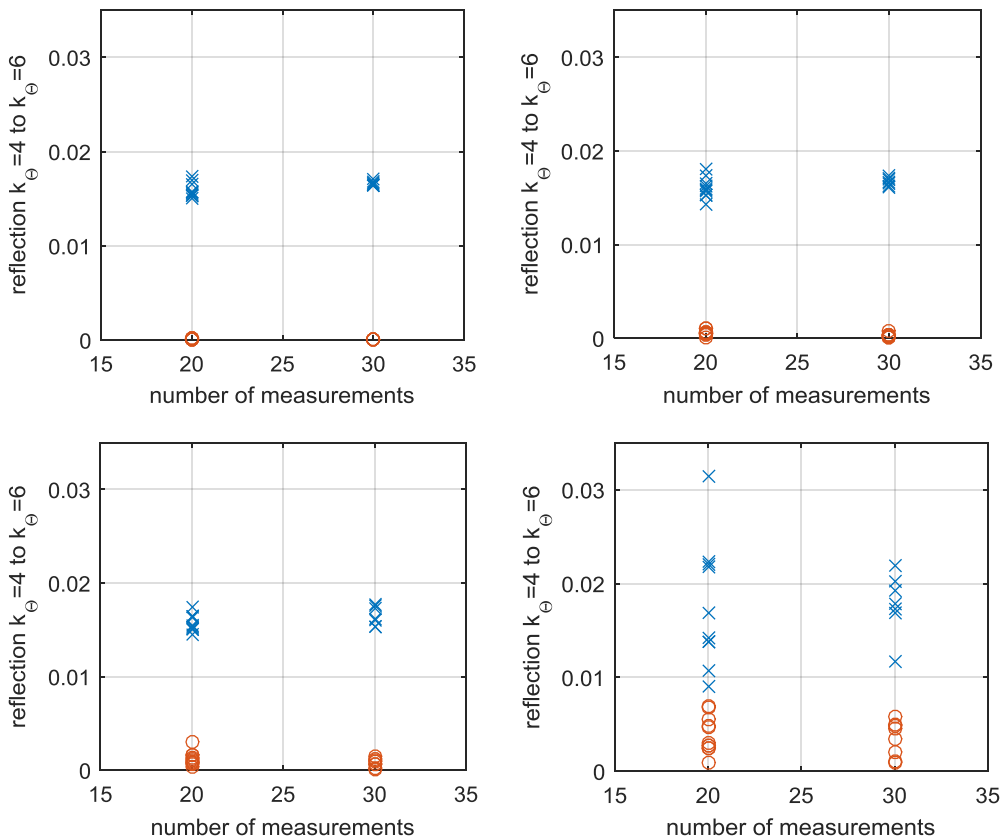


Figure 4: Reflection coefficient from the incident  $k_{\theta} = 4$  mode to the  $k_{\theta} = 6$  mode over the number of measurements used for calculating the scattering matrix (x with defect, o without defect). Standard deviation of measurement error 0.1% top left, 0.5% top right, 1% bottom left, 5% bottom right.

## 5 CONCLUSION

In this paper a method to calculate the scattering matrix based on measurements of the surface displacement of pipes is presented. An advantage of this approach over the standard ultrasonic guided wave technique is that the scattering of multiple modes at the defect can be captured at the same time, which leads to additional information about the defect itself. In addition, the effort to excite exactly one desired wavemode can be omitted, since this technique can handle a unknown excitations. On the other hand this technique is working in the frequency domain. Therefore the localization of the defect due to a time of flight measurement is not

possible, so that the defect needs to be within the measured area.

The second part of the paper dealt with the influence of the number of independent measurements included in the calculation procedure for the scattering matrix and the influence of random measurement noise. Although in theory it is sufficient to use a number of measurements equal to the number of incident wavemodes, a numerical study showed that the quality of the predicted scattering matrix can increase with the number of measurements included in the calculation.

Another numerical study indicated that the presented technique is rather robust to the influence of a random measurement error. In order to allow for the practical use of this technique further research needs to be undertaken, e.g. to identify the influence of the distribution and position of the measurement points on the pipe surface or the influence of the reflection at the ends of a finite pipe. Also additional experimental validation and a profound understanding of the scattering behavior of all incident wavemodes is necessary.

## 6 ACKNOWLEDGEMENTS

The European Commission is gratefully acknowledged for their support of the ANTARES project (GA606817). Furthermore, the authors acknowledge the financial support from Strategic Initiative Materials in Flanders (SIM) through the MADUROS, DEMOPROCI-NDT Program. The research of E. Deckers is funded by a grant from the Fund for Scientific Research – Flanders (F.W.O.). Also the Research Fund KU Leuven is gratefully acknowledged for its support. Additionally, this research was partially supported by Flanders Make.

## 7 REFERENCES

- [1] S. Cohn, "CNBC," 12 January 2011. [Online]. Available: <http://www.cnbc.com/id/41044074>. [Accessed 2016].
- [2] R. Carandente and P. Cawley, "The effect of complex defect profiles on the reflection of the fundamental torsional mode in pipes," *NDT & E International*, vol. 46, pp. 41-47, 2012.
- [3] B. Weinhacht, T. Klesse, R. Neubeck and L. Schubert, "Monitoring of hot pipes at the power plant Neurath using guided waves," in *SPIE Smart Structures and Materials+ Nondestructive Evaluation and Health Monitoring*, 2013.
- [4] P. Khalili and P. Cawley, "Excitation of Single Mode Lamb Waves at High Frequency Thickness Products.," *IEEE transactions on ultrasonics, ferroelectrics, and frequency control*, vol. 63, no. 2, pp. 303-312, 2015.
- [5] W. Böttger, H. Schneider and W. Weingarten, "Prototype EMAT system for tube inspection with guided ultrasonic waves," *Nuclear engineering and design*, vol. 102, no. 3, pp. 369-376, 1987.
- [6] W. Zhu and J. L. Rose, "Lamb wave generation and reception with time-delay periodic linear arrays: A BEM simulation and experimental study," *Ultrasonics, Ferroelectrics, and Frequency Control, IEEE Transactions on*, vol. 46, no. 3, pp. 654-664, 1999.
- [7] D. Alleyne and P. Cawley, "The long range detection of corrosion in pipes using Lamb waves," in *Review of progress in quantitative nondestructive evaluation*, vol. 14B, Springer, 1995, pp. 2073-2080.
- [8] D. Alleyne, M. Lowe and P. Cawley, "The reflection of guided waves from circumferential notches in pipes," *Journal of Applied mechanics*, vol. 65, no. 3, pp.

- 635-641, 1998.
- [9] A. Demma, P. Cawley, M. Lowe and A. Roosenbrand, "The reflection of the fundamental torsional mode from cracks and notches in pipes," *The Journal of the Acoustical Society of America*, vol. 114, no. 2, pp. 611-625, 2003.
  - [10] R. Carandente, J. Ma and P. Cawley, "The scattering of the fundamental torsional mode from axi-symmetric defects with varying depth profile in pipes," *The Journal of the Acoustical Society of America*, vol. 127, no. 6, pp. 3440-3448, 2010.
  - [11] A. Demma, P. Cawley, M. Lowe, A. Roosenbrand and B. Pavlakovic, "The reflection of guided waves from notches in pipes: a guide for interpreting corrosion measurements," *Ndt & E International*, vol. 37, no. 3, pp. 167-180, 2004.
  - [12] C.-Y. Kim and K.-J. Park, "Mode separation and characterization of torsional guided wave signals reflected from defects using chirplet transform," *NDT & E International*, vol. 74, pp. 15-23, 2015.
  - [13] E. Manconi and B. R. Mace, "Wave characterization of cylindrical and curved panels using a finite element method," *The Journal of the Acoustical Society of America*, vol. 125, no. 1, pp. 154-163, 2009.
  - [14] E. Manconi and B. Mace, "Modelling wave propagation in two-dimensional structures using a wave/finite element technique," *ISVR Technical Memorandum 966*, 2007.
  - [15] J. M. Renno and B. R. Mace, "Calculating the forced response of cylinders and cylindrical shells using the wave and finite element method," *Journal of Sound and Vibration*, vol. 333, no. 21, pp. 5340-5355, 2014.
  - [16] W. Zhou, M. Ichchou and J. Mencik, "Analysis of wave propagation in cylindrical pipes with local inhomogeneities," *Journal of Sound and Vibration*, vol. 319, no. 1, pp. 335-354, 2009.
  - [17] J. M. Renno and B. R. Mace, "Calculation of reflection and transmission coefficients of joints using a hybrid finite element/wave and finite element approach," *Journal of Sound and Vibration*, vol. 332, no. 9, pp. 2149-2164, 2013.